

Short Communication

Numerical Analysis on the Effect of Stoichiometric Ratio on Fuel Utilization and Performance of High Temperature Proton Exchange Membrane Fuel Cells

Shian Li¹, Rongqiang Wei¹, Xinrong Lv¹, Weiqiang Ye², Qiuwan Shen^{1,*}, Guogang Yang^{1,*}

¹ Marine Engineering College, Dalian Maritime University, China.

² Marine Engineering College, Guangzhou Maritime University, China.

*E-mail: shenqiuwan@dlnu.edu.cn and yanggg@dlnu.edu.cn

Received: 9 April 2020 / Accepted: 25 May 2020 / Published: 10 July 2020

A three-dimensional mathematical model is developed and then employed to examine the effect of stoichiometric ratio on fuel utilization of high temperature proton exchange membrane fuel cells. The effect of stoichiometric ratio on cell performance and transport phenomena is also investigated. The performance of fuel cells at different stoichiometric ratios are obtained and compared. It is found that the cell performance can be improved by increasing the stoichiometric ratio, but it can not be continually increased. And the heat, mass and charge transport processes of fuel cells at different stoichiometric ratios are also presented and compared.

Keywords: High temperature proton exchange membrane fuel cells, Stoichiometric ratio, Fuel utilization, Cell performance, Transport characteristics

1. INTRODUCTION

Low temperature proton exchange membrane fuel cells (LT-PEMFCs) operate at relatively low temperature (<100 °C), and the thermal and water management strategies are needed due to the existence of liquid water [1-4]. Meanwhile, high temperature proton exchange membrane fuel cells (HT-PEMFCs) have already been proposed. In comparison with LT-PEMFCs, HT-PEMFCs have the following advantages: high CO tolerance, fast reaction kinetics and easy water management [5-6].

Numerical and experimental studies were reported in the open literature. A two-dimensional model was extended to a three-dimensional model to examine the transport phenomena inside fuel cells [7-8]. The fuel cells with coolant channels and gas crossover were extensively studied by Chippar and Ju [9-10]. And the effects of the operating temperature [11-12], novel membrane types [13-14] and

flow field designs [15-19] on performance were extensively investigated. Numerical investigations were carried out to study the effect of membrane conductivity on cell performance [20].

However, an isothermal model was commonly employed to investigate the transport phenomena and cell performance [20]. Therefore, it is necessary to improve the understanding of the transport characteristics inside fuel cells by using a non-isothermal model. In the present work, a three-dimensional, non-isothermal model including the mass, momentum, species, energy and charge equations is developed and then employed to examine the effect of stoichiometric ratio on fuel utilization. The performance of fuel cells at different stoichiometric ratios are obtained and compared. In addition, the distributions of species, temperature, and local current density of the corresponding cases are shown and analyzed.

2. MATHEMATICAL MODEL DESCRIPTION

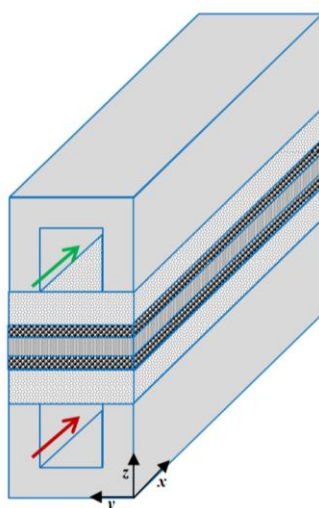


Figure 1. Computational domain of the present study.

Table 1. Geometric parameters and operating conditions of this study.

Parameters	Value	Units
Cell length	100	mm
Cell width	2	mm
FC width	1	mm
FC height	1	mm
CC rib width	1	mm
CC height	1.5	mm
GDL thickness	0.2	mm
CL thickness	0.01	mm
Membrane thickness	0.05	mm
Operating pressure, P_a/P_c	1/1	atm
Operating temperature, T_a/T_c	443/443	K

As shown in Figure 1, the computational domain consists of the anode/cathode current collectors (CCs), flow channels (FCs), gas diffusion layers (GDLs), catalyst layers (CLs) and membrane. The corresponding geometric parameters and operating conditions are shown in Table 1. Dry hydrogen and air are fed into the FCs with co-flow arrangement. The operating temperature is 443 K and operating pressure is 1.0 atm. The stoichiometric ratios of 1.0, 2.0 and 3.0 are used in this study.

2.1 Governing equations

The governing equations and corresponding source terms are given in Table 2 and Table 3, respectively. The following assumptions are used in the present mathematical model. The fluid flow is single phase and laminar flow. Ideal gas mixture is applied. The electrodes are isotropic and homogeneous. And the contact resistance is neglected. The detailed descriptions of parameters can be found in our previous studies [17-18].

Table 2. Governing equations of the mathematical model.

Species conservation equation:	$\nabla \cdot (\rho \vec{u}) = S_{mass}$
Momentum conservation equation:	$\nabla \cdot (\rho \vec{u} \vec{u}) = \nabla \cdot (\mu \nabla \vec{u}) - \nabla P + S_{mom}$
Species conservation equation:	$\nabla \cdot (\rho \vec{u} Y_i) = \nabla \cdot (\rho D_{eff,i} \nabla Y_i) + S_i$
Energy conservation equation:	$\nabla \cdot (\rho c_p \vec{u} T) = \nabla \cdot (k_{eff} \nabla T) + S_T$
Charge conservation equation:	$\nabla \cdot (\sigma_{eff,s} \nabla \phi_s) + S_s = 0$
	$\nabla \cdot (\sigma_{eff,m} \nabla \phi_m) + S_m = 0$

2.2 Numerical implementation and boundary conditions

Table 3. Source terms of the governing equations.

Description	Units
$S_{mass} = S_{H_2}$ (Anode CL)	$\text{kg m}^{-3} \text{s}^{-1}$
$S_{mass} = S_{O_2}$ (Cathode CL)	
$S_{mass} = S_{H_2O}$ (Cathode CL)	
$S_{mom} = -\frac{\mu}{K} \vec{u}$ (Anode/Cathode GDL and CL)	$\text{kg m}^{-2} \text{s}^{-2}$
$S_{H_2} = -\frac{j_a}{2F} M_{H_2}$ (Anode CL)	$\text{kg m}^{-3} \text{s}^{-1}$
$S_{O_2} = -\frac{j_c}{4F} M_{O_2}$ (Cathode CL)	$\text{kg m}^{-3} \text{s}^{-1}$
$S_{H_2O} = \frac{j_c}{2F} M_{H_2O}$ (Cathode CL)	$\text{kg m}^{-3} \text{s}^{-1}$

$$\begin{aligned}
 S_T &= j_a |\eta_a| + \sigma_{eff,m} \|\nabla \phi_m\|^2 + \sigma_{eff,s} \|\nabla \phi_s\|^2 \text{ (Anode CL)} && \text{W m}^{-3} \\
 S_T &= j_c |\eta_c| - j_c \frac{dU_0}{dT} T + \sigma_{eff,m} \|\nabla \phi_m\|^2 + \sigma_{eff,s} \|\nabla \phi_s\|^2 \text{ (Cathode CL)} \\
 S_T &= \sigma_{eff,m} \|\nabla \phi_m\|^2 \text{ (Membrane)} \\
 S_T &= \sigma_{eff,s} \|\nabla \phi_s\|^2 \text{ (Anode/Cathode GDL)} \\
 S_s &= -j_a \text{ (Anode CL)} && \text{A m}^{-3} \\
 S_s &= +j_c \text{ (Cathode CL)} \\
 S_m &= +j_a \text{ (Anode CL)} && \text{A m}^{-3} \\
 S_m &= -j_c \text{ (Cathode CL)}
 \end{aligned}$$

The fuel cell model is implemented by using the ANSYS FLUENT. The SIMPLE algorithm is adopted for the coupling of pressure and velocity fields. The second order upwind discretization scheme is used for the governing equations to ensure the calculation accuracy. The mass flow rate of hydrogen/air, operating temperature, and mass fraction are prescribed at the inlet of anode/cathode FCs. The mass flow rate is calculated at a reference current density of 1.0 A/cm². A pressure-outlet condition is assigned at the outlet of FCs. At the anode and cathode terminals, temperature and electric potential are specified. When a cell voltage is given, the corresponding current density can be obtained after the numerical computation.

3. RESULTS AND DISCUSSION

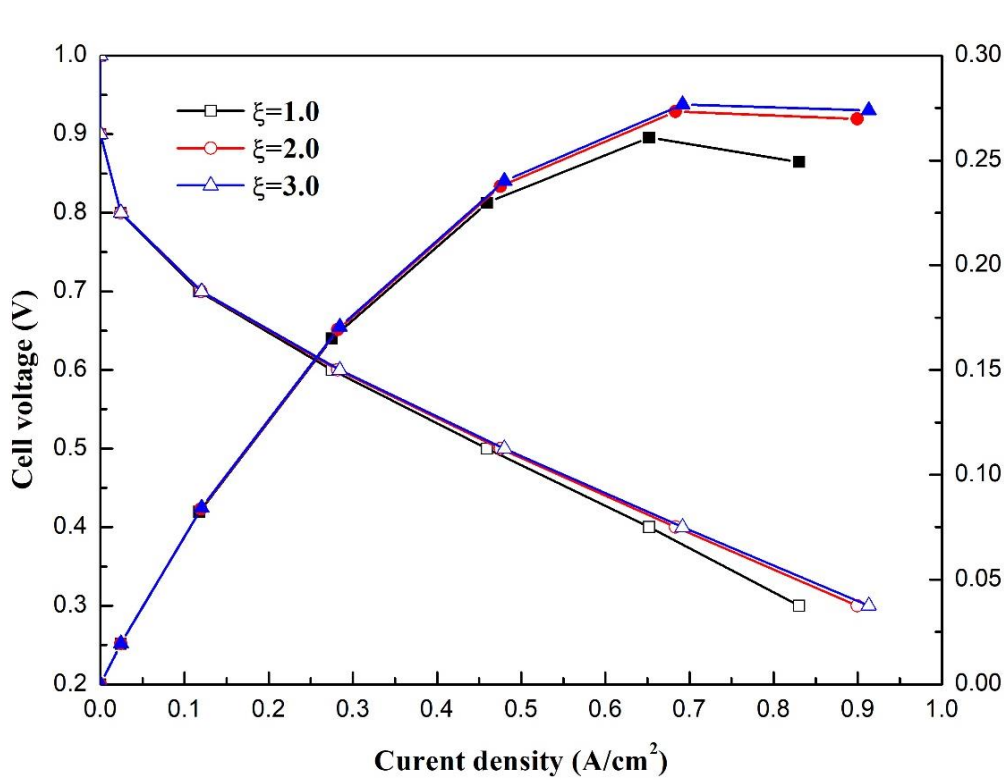


Figure 2. Effect of stoichiometric ratio on cell performance.

Numerical simulations have already been extensively used to improve the understanding of HT-PEMFCs [21]. A three-dimensional model can accurately predict the transport processes inside fuel cells compared to one-dimensional and two-dimensional models [22]. The transport processes are related to the temperature distributions, so the energy equation must be included in the mathematical model. A three-dimensional and non-isothermal mathematical model including the mass, momentum, species, energy and charge equations is developed and then employed to examine the effect of stoichiometric ratio on cell performance and fuel utilization. The stoichiometric ratios of 1.0, 2.0 and 3.0 are used in this study. The effect of stoichiometric ratio on performance of fuel cells is shown in Figure. 2. It is clear that performance is greatly enhanced as the at the stoichiometric ratio changes from 1.0 to 2.0, especially at low cell voltages. But the cell performance is only slightly enhanced when the stoichiometric ratio ranges from 2.0 to 3.0. And the cell performance is not affected by the stoichiometric ratio at high cell voltages. This indicates that the cell performance can not be continually increased by increasing the stoichiometric ratio. At cell voltage 0.3 V, the current densities of three cases are 0.831 A/cm², 0.899 A/cm² and 0.913 A/cm², respectively. And the corresponding power densities are 0.249 W/cm², 0.269 W/cm² and 0.274 W/cm², respectively.

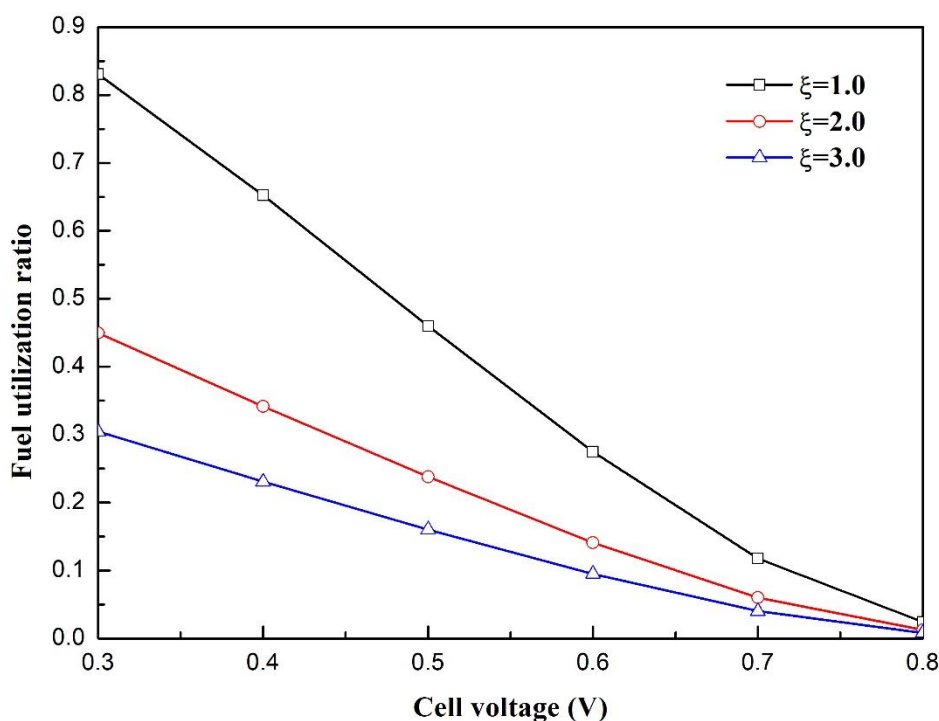


Figure 3. Effect of stoichiometric ratio on fuel utilization.

The mass flow rate prescribed at the inlet of FCs is calculated at a reference current density of 1.0 A/cm². The effect of stoichiometric ratio on fuel utilization of fuel cells is shown in Figure. 3. It can be observed that the fuel utilization is increased when the cell voltage is decreased. At the same cell voltage, the fuel utilization is decreased with increasing stoichiometric ratio. At the cell 0.3V, the fuel utilization ratios of three cases are 0.83, 0.45 and 0.3, respectively. This indicates that the

consumption amount of fuel can not be greatly increased when the stoichiometric ratio keeps increasing. This is consistent with the results shown in Figure 2.

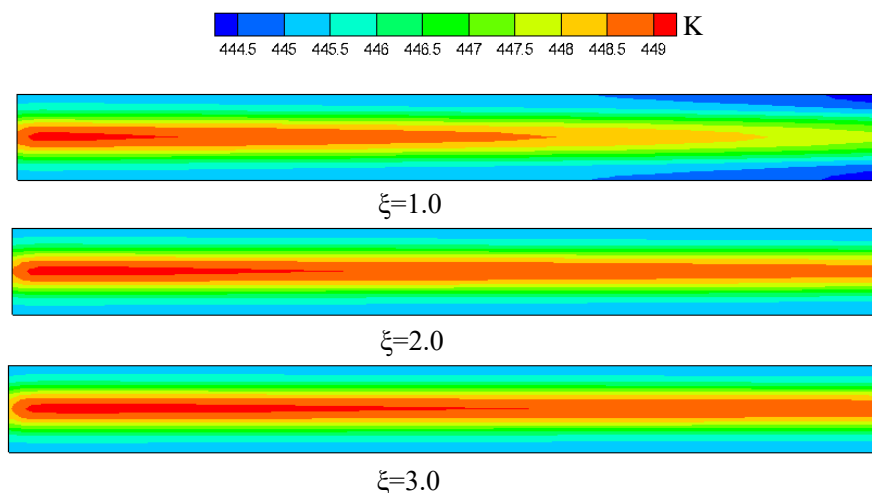


Figure 4. Effect of stoichiometric ratio on temperature distribution at cell voltage 0.3 V.

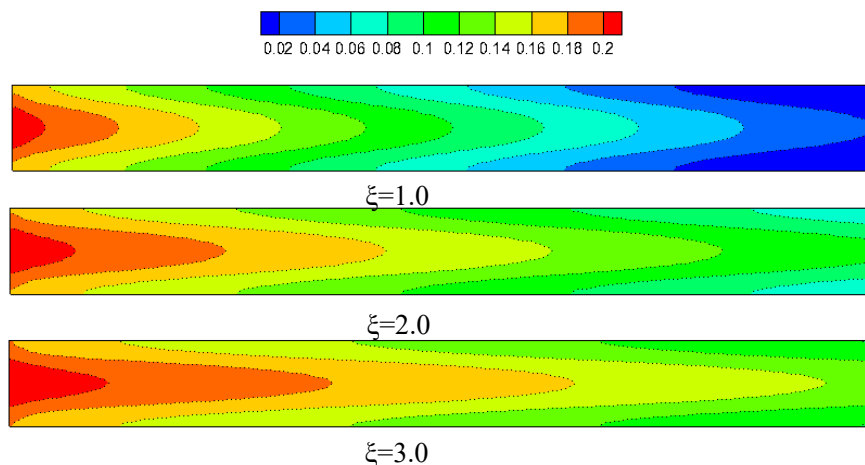


Figure 5. Effect of stoichiometric ratio on oxygen mass fraction distribution at cell voltage 0.3 V.

The effect of stoichiometric ratio on local transport characteristics is investigated in the following sections. The effect of stoichiometric ratio on temperature distribution of the cathode CL and membrane interface at cell voltage 0.3 V is presented in Figure 4. The temperature becomes small along the flow direction for the case with the stoichiometric ratio of 1.0. This is attributed to insufficient supply of reactants from the FCs. And the amount of generated heat becomes small. When the stoichiometric ratio is increased to 2.0, the supply of reactants is sufficient for the electrochemical reactions. The temperature is just slightly changed along the flow direction. The similar temperature distribution is also observed in the case with the stoichiometric ratio of 3.0. As shown in Figures 5-6, the effect of stoichiometric ratio on oxygen and water mass fraction distribution of the GDL and CL

interface at cell voltage 0.3 V is presented. The oxygen mass fraction is gradually decreased and water mass fraction is gradually increased along the flow direction due to the consumption of oxygen and production of water. A relative low oxygen mass fraction and high water mass fraction distributions are observed at the downstream of fuel cell due to a small stoichiometric ratio.

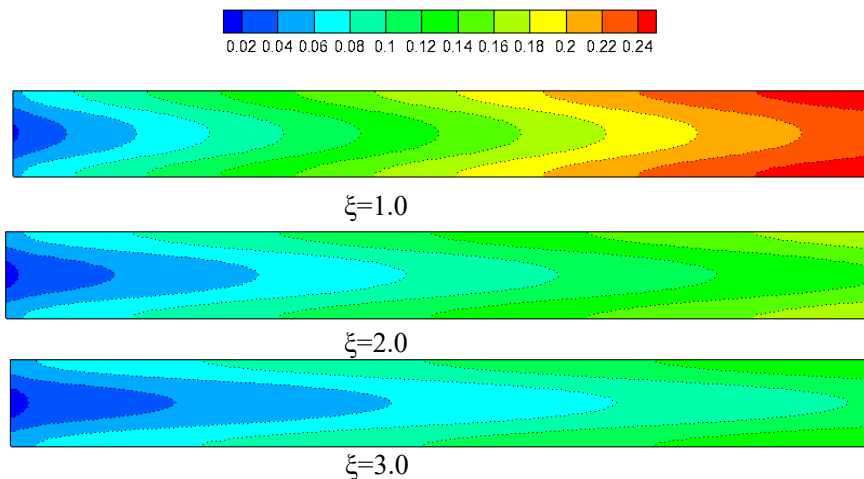


Figure 6. Effect of stoichiometric ratio on water mass fraction distribution at cell voltage 0.3 V.

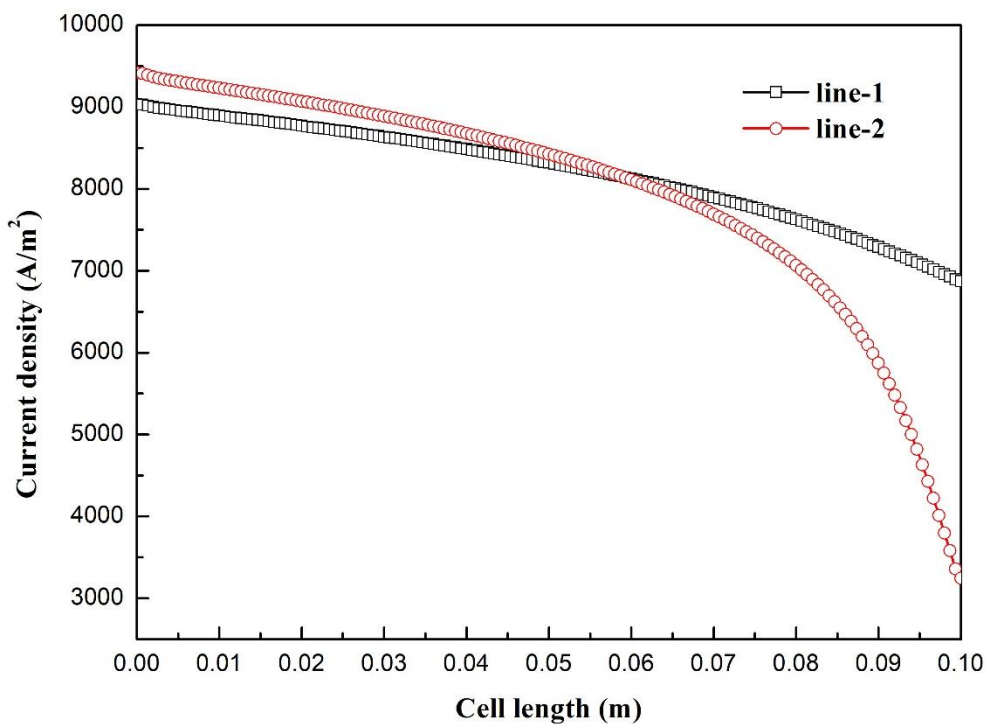


Figure 7. Local current density of the fuel cell with the stoichiometric ratio of 1.0 at cell voltage 0.3 V.

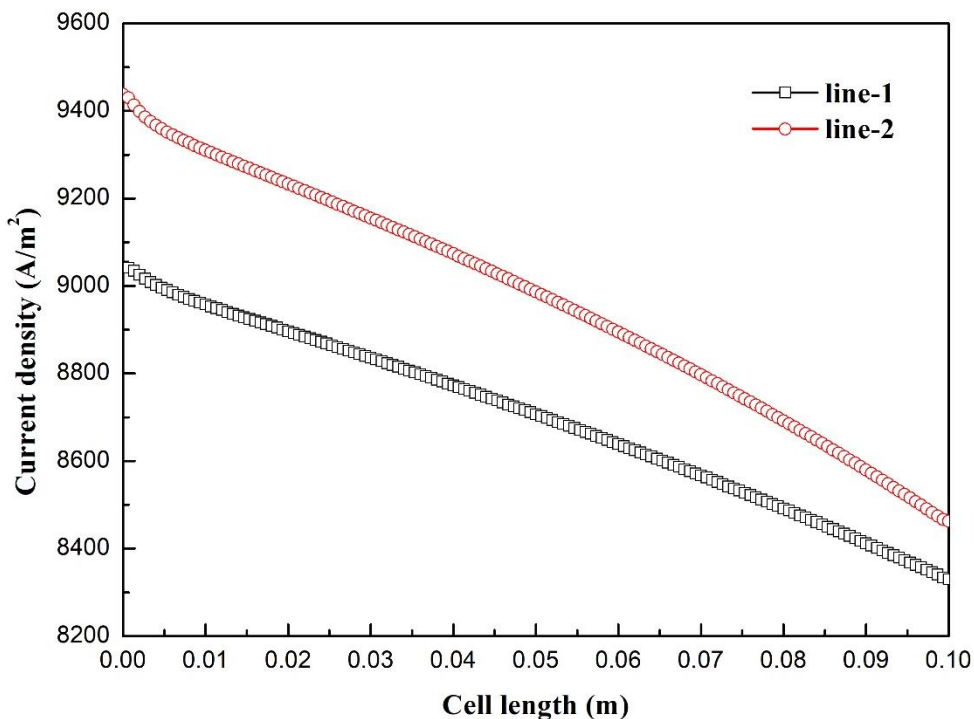


Figure 8. Local current density of the fuel cell with the stoichiometric ratio of 2.0 at cell voltage 0.3 V.

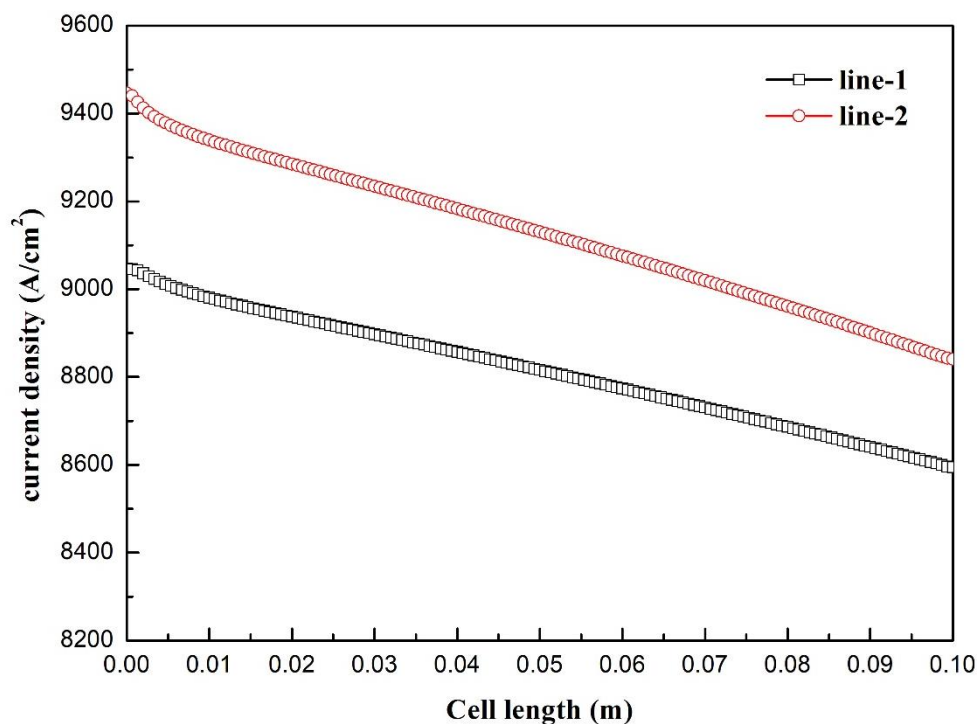


Figure 9. Local current density of the fuel cell with the stoichiometric ratio of 3.0 at cell voltage 0.3 V.

The effect of stoichiometric ratio on local current density distribution of fuel cell at cell voltage 0.3 V is shown in Figures 7-9. It is clearly seen that the local current density is strongly affected by the

stoichiometric ratio. Line-1 is the position of $y=0.0001$ m, and line-2 is the position of $y=0$ m. For the case with the stoichiometric ratio of 1.0, the current density at the position of line-2 is sharply decreased from the middle of fuel cell. And the current density at the position of line-1 is gradually decreased along the flow direction. For the case with the stoichiometric ratio of 2.0, the reduction of current density at the position of line-2 is larger than that at the position of line-1. For the case with the stoichiometric ratio of 3.0, the reduction of current density at the position of line-2 is almost the same as that at the position of line-1. These can be attributed to the distributions of reactants caused by the different stoichiometric ratios.

4. CONCLUSIONS

A three-dimensional, non-isothermal model was used to study the effect of stoichiometric ratio on fuel utilization of high temperature proton exchange membrane fuel cells. The fuel utilization is increased when the cell voltage is decreased. At the same cell voltage, the fuel utilization is decreased with increasing stoichiometric ratio. The cell performance is greatly improved as the at the stoichiometric ratio changes from 1.0 to 2.0, especially at low cell voltages. But the cell performance is only slightly enhanced when the stoichiometric ratio ranges from 2.0 to 3.0. In addition, the distributions of temperature, oxygen mass fraction, water mass fraction and local current density are also strongly affected by the stoichiometric ratio. These result from the amount of reactants supplied into fuel cells. The results improve the understanding on fuel utilization and performance of high temperature proton exchange membrane fuel cells with different stoichiometric ratios.

ACKNOWLEDGMENTS

The authors gratefully acknowledge the financial supports from National Natural Science Foundation of China (No.51779025). This work is also funded by the Fundamental Research Funds for the Central Universities of China (No. 3132019327), China Postdoctoral Science Foundation (No.2019M651097 and No.2019M651094), Natural Science Foundation of Liaoning Province (No.2019-BS-026 and No.2019-ZD-0154), Innovation and Start-up Business Education Project of Universities in Guangzhou (2019PT201) and Innovative strong School Project of Guangzhou Maritime University (F410102).

References

1. F. Nandjou, J.P. Crouvezier, M. Chandesris, J.F. Blachot, C. Bonnaud, Y. Bultel, *J. Power Sources*, 326 (2016) 182.
2. T.D. Tran, S. Huang, D.H. Vu, V.N. Duy, *Int. J. Electrochem. Sci.*, 13 (2018) 10480.
3. S.A. Li, R.Q. Wei, Y.X. Qi, G.G. Yang, Q.W. Shen, *Int. J. Electrochem. Sci.*, 14 (2019) 11367.
4. S.A. Li, R.Q. Wei, G.L. Zhang, Y.X. Qi, G.G. Yang, Q.W. Shen, *Int. J. Electrochem. Sci.*, 15 (2020) 4138.
5. S.S. Araya, F. Zhou, V. Liso, S.L. Sahlin, J.R. Vang, S. Thomas, X. Gao, C. Jeppesen, S.K. Kaer, *Int. J. Hydrogen Energy*, 41 (2016) 21310.
6. R.K.A. Rasheed, Q. Liao, C.Z. Zhang, S.H. Chan, *Int. J. Hydrogen Energy*, 42 (2017) 3142.
7. D.F. Cheddie, N.D.H. Munroe, *Int. J. Hydrogen Energy*, 32 (2007) 832.
8. D.F. Cheddie, N.D.H. Munroe, *J. Power Sources*, 160 (2006) 215.

9. P. Chippar, H. Ju, *Solid state Ion.*, 225 (2012) 30.
10. P. Chippar, H. Ju, *Int. J. Hydrogen Energy*, 38 (2013) 7704.
11. G. Elden, M. Celik, G. Genc, H. Yapici, *Energy*, 103 (2016) 772.
12. D.G. Caglayan, B. Sezgin, Y. Devrim, I. Eroglu, *Int. J. Hydrogen Energy*, 41 (2016) 10060.
13. S. Matar, A. Higier, H.T. Liu, *J. Power Sources*, 195 (2010) 181.
14. H. Sun, C. Xie, H. Chen, S. Almheiri, *Appli. Energy*, 160 (2015) 937.
15. R. Taccani, N. Zuliani, *Int. J. Hydrogen Energy*, 36 (2011) 10282.
16. D. Singdeo, T. Dey, S. Gaikwad, S.J. Andreasen, P.C. Ghosh, *Appli. Energy*, 195 (2017) 13.
17. S.A. Li, J. L. Yuan, G.N. Xie, B. Sunden, *Numer. Heat Transfer A*, 72 (2017) 807.
18. S.A. Li, B. Sunden, *Int. J. Hydrogen Energy*, 42 (2017) 27323.
19. S.W. Perng, H.W. Wu, Y.B. Chen, Y.K. Zeng, *Appli. Energy*, 255 (2019) 113815.
20. B. Sezgin, D.G. Caglayan, Y. Devrim, T. Steenberg, I. Eroglu, *Int. J. Hydrogen Energy*, 41 (2016) 10001.
21. R.K.A. Rasheed, Q. Liao, C. Zhang, S.H. Chan, *Int. J. Hydrogen Energy*, 42 (2017) 3142.
22. Y. Nalbant, C.O. Colpan, Y. Devrim, *Int. J. Hydrogen Energy*, 43 (2018) 5939.

© 2020 The Authors. Published by ESG (www.electrochemsci.org). This article is an open access article distributed under the terms and conditions of the Creative Commons Attribution license (<http://creativecommons.org/licenses/by/4.0/>).